

Structural Isomers of $\{\text{Mn}^{\text{II}}(\text{L})_2[\text{Ag}^{\text{I}}(\text{CN})_2]_2\}$ (L = 3-Methylpyridine or 4-Methylpyridine), Bilayer Structure with Binuclear Argentophilic Interaction and Interpenetrated Structure with 1D Chain Argentophilic Interaction; Synthesis, Crystal Structure, and Magnetic Properties

Takashi Kosone,¹ Yusuke Suzuki,¹ Chikahide Kanadani,^{2,3}
Toshiaki Saito,^{2,3} and Takafumi Kitazawa^{*1,2}

¹Department of Chemistry, Faculty of Science, Toho University, 2-2-1 Miyama, Funabashi 274-8510

²Research Center for Materials with Integrated Properties, Toho University, 2-2-1 Miyama, Funabashi 274-8510

³Department of Physics, Faculty of Science, Toho University, 2-2-1 Miyama, Funabashi 274-8510

Received July 7, 2008; E-mail: kitazawa@chem.sci.toho-u.ac.jp

New novel 2D network bimetallic $\text{Mn}^{\text{II}}\text{Ag}^{\text{I}}$ coordination compounds $\{\text{Mn}^{\text{II}}(\text{L})_2[\text{Ag}^{\text{I}}(\text{CN})_2]_2\}_n$ (L = 3-methylpyridine (**1**) or 4-methylpyridine (**2**)) were synthesized and characterized by using single-crystal X-ray analysis and magnetic measurements. Mn^{II} ion in both complexes has MnN_6 coordination with octahedral geometries, which are linked by a $[\text{Ag}^{\text{I}}(\text{CN})_2]^-$ unit at the equatorial plane to form a polymeric 2D sheet architecture. The two pyridine rings coordinate at the axial positions. However, coordination polymers for **1** and **2** are structural isomers. The structure of **1** comprises a parallel 2D array and the layers interact by pairs defining bilayers with strong binuclear argentophilic interaction, while **2** comprises a double interpenetration structure with 1D-chain weak argentophilic interaction. Furthermore, intermolecular C...C contacts in these complexes are significantly smaller than the sum of the van der Waals radius. Variable-temperature (2–300 K) magnetic susceptibility measurements of both the compounds have been performed to understand the possibility of spin transition in **1** and **2**. However, the susceptibility data of **1** and **2** indicate the existence of high-spin (HS) state manganese(II) throughout the temperature range.

Polynuclear coordination compounds, in which the metal centers self-assemble from organic linkers to display a variety of supramolecular architectures are currently evolving a great deal of research due to their intriguing metal–organic framework (MOFs) topologies and their potential uses in molecular devices, nonlinear optics, porous materials, and other applications. Polycyanometalates are useful building blocks for various kinds of coordination polymeric networks with useful functional properties, such as clathrate hosts,¹ spin-crossover phenomena,^{2–7} and molecular magnets.⁸ Among the synthetic strategies for cyano-bridged coordination networks, dicyanometalates $[\text{M}^{\text{I}}(\text{CN})_2]^-$ (M = Ag and Au) with linear coordination geometries have been used as building blocks, because they can link coordination metal centers, through the N atoms of the bidentate CN substituents.

Examples of coordination polymers built with a dicyanometalate are $\{\text{M}^{\text{II}}(\text{py})_2[\text{M}'^{\text{I}}(\text{CN})_2]_2\}$ (M = Fe and Cd) (M' = Ag and Au) (py = pyridine).^{1a,3b,3d} These complexes are isostructural to each other and construct two-dimensional (2D) $\{\text{M}^{\text{II}}[\text{Ag}^{\text{I}}(\text{CN})_2]_2\}$ sheet network structures, including the large rhombus $\{\text{M}^{\text{II}}_4[\text{Ag}^{\text{I}}(\text{CN})_2]_4\}$, which are called Hofmann-like structures. In particular, $\{\text{Fe}(\text{py})_2[\text{Ag}^{\text{I}}(\text{CN})_2]_2\}$ and $\{\text{Fe}(\text{py})_2[\text{Au}^{\text{I}}(\text{CN})_2]_2\}$ undergo spin-crossover phase transition.^{3b,3d} We have developed a synthetic route to prepare several Hofmann-like cyano-bridged coordination polymers with pyridine derivatives. Another interesting feature of some

of these silver and gold compounds is the metallophilic interactions.^{1,4–7,9–11} Metallophilicity is a closed-shell intermolecular interaction between silver(I) or gold(I) atoms.¹² The interactions are comparable to hydrogen bonds.^{11,12} In the case of silver, the attraction has been called an argentophilic interaction. Some octahedral $\text{Fe}^{\text{II}}-[\text{Ag}^{\text{I}}(\text{CN})_2]$ compounds, such as $\{\text{Fe}^{\text{II}}(\text{py})_2[\text{Ag}^{\text{I}}(\text{CN})_2]_2\}$, exhibit spin-crossover phenomena. The crystal structures of octahedral $\text{Mn}^{\text{II}}-[\text{Ag}^{\text{I}}(\text{CN})_2]$ compounds are similar to that of $\text{Fe}^{\text{II}}-[\text{Ag}^{\text{I}}(\text{CN})_2]$.^{4,13} Many Hofmann-like compounds $\{\text{Fe}(3\text{-Xpy})_2[\text{M}(\text{CN})_2]_2\}$ (X = CN, F, Cl, Br, and I) (M = Ag and Au) have been reported,^{3c,6,14} but Mn^{II} ions in place of Fe^{II} ions have been little investigated.

In this work, we report the synthesis, crystal structure, and magnetic properties of novel bimetallic coordination polymers with the formula $\{\text{Mn}^{\text{II}}(\text{L})_2[\text{Ag}^{\text{I}}(\text{CN})_2]_2\}_n$ (L = 3-methylpyridine (**1**) or 4-methylpyridine (**2**)).

Experimental

Materials. All the chemicals were purchased from commercial sources and used without any further purification.

Synthesis. In 10 mL of water, $\text{MnCl}_2 \cdot 4\text{H}_2\text{O}$ (0.02 g, 0.1 mmol) and $\text{K}[\text{Ag}(\text{CN})_2]$ (0.04 g, 0.2 mmol) were dissolved. Vapor diffusion using 3-methylpyridine or 4-methylpyridine as a source of ligand molecules provided colorless polycrystalline crystals suitable for X-ray diffraction of **1** and **2** over a period of two days. Yield: 0.023 g (41%) for **1**, 0.031 g (55%) for **2**. **1**: Anal. Calcd for

Table 1. Crystal Data

Crystal data	1	2
Empirical formula	$C_{16}H_{14}Ag_2MnN_6$	$C_{16}H_{14}Ag_2MnN_6$
FW	561.01	561.01
Temperature/K	293	293
Crystal system	Monoclinic	Tetragonal
Space group	$P2_1/n$	$I4_1$
$a/\text{\AA}$	9.5395(5)	12.0788(3)
$b/\text{\AA}$	14.3539(7)	12.0788(3)
$c/\text{\AA}$	15.7069(8)	13.4674(6)
$\beta/^\circ$	105.6430(10)	—
$V/\text{\AA}^3$	2071.07(18)	1964.86(11)
Z	4	4
$d_{\text{calcd}}/\text{Mg m}^{-3}$	1.799	1.896
Absorption coefficient $/\text{mm}^{-1}$	2.482	2.616
$F(000)$	1084	1084
Crystal size/ mm^3	$0.30 \times 0.30 \times 0.30$	$0.30 \times 0.30 \times 0.30$
Reflections collected	13185	7387
Independent	4912	2799
Reflections	$[R(\text{int}) = 0.0224]$	$[R(\text{int}) = 0.0288]$
GOF on F^2	1.077	1.167
$R1, {}^a wR2^b$	0.0270, 0.0478	0.0374, 0.0880
Largest diff. peak and hole/ $e \text{\AA}^{-3}$	0.407 and -0.911	0.441 and -2.495

a) $R1 = (\sum ||F_o| - |F_c||) / \sum |F_o|$. b) $wR2 = \{\sum w(|F_o| - |F_c|)^2 / \sum w|F_o|^2\}^{1/2}$.

C, 34.26; H, 2.52; N, 14.98%. Found: C, 34.17; H, 2.47; N, 14.98%. IR (nujol method, cm^{-1}): 2156 ($\nu_{\text{CN}}(\text{CN})$). **2**: Anal. Calcd for C, 34.26; H, 2.52; N, 14.98%. Found: C, 34.13; H, 2.57; N, 14.97%. IR (nujol, cm^{-1}): 2152 (ν_{CN}).

Structure Determination. Crystal structures of the two complexes were determined using a BRUKER APEX SMART CCD area-detector diffractometer with monochromated $\text{Mo K}\alpha$ radiation ($\lambda = 0.71073 \text{\AA}$). The diffraction data were treated using SMART and SAINT, and absorption correction was performed using SADABS.¹⁵ The structures were solved by using direct methods with SHELXTL.¹⁶ All non-hydrogen atoms were refined anisotropically, and the hydrogen atoms were generated geometrically. Pertinent crystallographic parameters are displayed in Table 1 and selected metric parameters for the complexes are presented in Table 2. Crystallographic data have been deposited with Cambridge Crystallographic Data Centre: Deposition numbers CCDC-692264 for compound No. 1 and CCDC-692265 for compound No. 2. Copies of the data can be obtained free of charge via <http://www.ccdc.cam.ac.uk/conts/retrieving.html> (or from the Cambridge Crystallographic Data Centre, 12, Union Road, Cambridge, CB2 1EZ, U.K.; Fax: +44 1223 336033; e-mail: deposit@ccdc.cam.ac.uk).

Magnetic Measurement. Measurements of the temperature dependence of the magnetic susceptibility of the two complexes in the temperature range of 2–300 K with a cooling and heating rate of 1 K min^{-1} in a 1 kOe field were measured on a MPMS-XL Quantum Design SQUID magnetometer.

Results and Discussion

Synthesis and IR Spectra. The reaction of an aqueous solution of $\text{MnCl}_2 \cdot 4\text{H}_2\text{O}$ containing two equivalents of $\text{K}[\text{Ag}(\text{CN})_2]$ with a vapor diffusion method using pyridine-

Table 2. Selected Bond Lengths and Angles

1	2
Bond lengths/ \AA	
Mn(1)–N(1)	2.316(3)
Mn(1)–N(2)	2.312(3)
Mn(1)–N(3)	2.217(3)
Mn(1)–N(4)	2.235(2)
Mn(1)–N(5)	2.232(3)
Mn(1)–N(6)	2.231(3)
Ag(1)–C(11)	2.058(3)
Ag(1)–C(12)	2.052(4)
Ag(2)–C(13)	2.052(4)
Ag(2)–C(14)	2.050(4)
Bond angles/ $^\circ$	
N(1)–Mn(1)–N(2)	172.68(10)
N(3)–Mn(1)–N(5)	177.58(12)
N(4)–Mn(1)–N(6)	177.51(12)
N(1)–Mn(1)–N(3)	90.13(11)
N(1)–Mn(1)–N(4)	85.36(11)
N(2)–Mn(1)–N(5)	90.62(11)
N(2)–Mn(1)–N(6)	90.54(11)
C(14)–N(3)–Mn(1)	173.9(3)
C(13)–N(4)–Mn(1)	170.3(3)
C(11)–N(5)–Mn(1)	172.8(3)
C(12)–N(6)–Mn(1)	173.3(3)
C(11)–Ag(1)–C(12)	176.14(16)
C(13)–Ag(2)–C(14)	178.98(16)

derivative ligand ($L = 3\text{-methylpyridine}$ or 4-methylpyridine) afforded crystals of the 2D cyano-bridged coordination polymers $\{Mn^{II}(L)_2[Ag^I(CN)_2]_n\}$ ($L = 3\text{-methylpyridine}$ (**1**) or 4-methylpyridine (**2**)).

The solid-state IR spectra of **1** and **2** had $\text{C}\equiv\text{N}$ bands at 2156 cm^{-1} for **1** and 2152 cm^{-1} for **2**, which are both at higher wavenumbers than that of free $[\text{Ag}(\text{CN})_2]^-$ (2135 cm^{-1}), at room temperature. This suggests that both of the CN groups of $[\text{Ag}(\text{CN})_2]^-$ act as bidentate bridging ligands.

Crystal Structure. Coordination compounds **1** and **2** crystallized in the centrosymmetric space groups $P2_1/n$ and $I4_1$, respectively. Two-dimensional frameworks of **1** and **2** are shown in Figure 1. The $[\text{Mn}^{II}\text{Ag}^I(\text{CN})_2]_4$ rectangular mesh network is bent. The coordination environment of the Mn^{II} ions and Ag^I atoms in complex **2** are similar to those of **1**. There is one type of manganese ion Mn(1) which lies on an inversion center with an N_6 coordination sphere. Four N atoms from bidentate cyano substituents are coordinated to Mn^{II} atoms in the equatorial positions. Complex **1** has two types of crystallographically distinct almost linear $[\text{Ag}(\text{CN})_2]^-$ units while complex **2** has one type of crystallographically distinct almost linear $[\text{Ag}(\text{CN})_2]^-$ unit (Figure 2). The angles for **1** defined by C(11)–Ag(1)–C(12) and C(13)–Ag(2)–C(14) are, respectively, $176.14(16)$ and $178.98(16)$ and for **2** defined by C(7)–Ag(1)–C(8) is $178.82(17)$. The pyridyl nitrogen ligation site at the two 3-methylpyridine or 4-methylpyridine ligands coordinates in the axial positions of Mn(1) (Figure 2). The $\text{N}_{\text{py}}\text{--Mn(1)}\text{--N}_{\text{py}}$ angle for complex **2** is perfectly linear, but complex **1** is bent ($172.68(10)$). The Mn...Mn distances in the Mn(1)–NC–Ag(1)–

CN–Mn(1) and Mn(1)–NC–Ag(2)–CN–Mn(1) one-dimensional wave chain edges for **1** and Mn(1)–NC–Ag(1)–CN–Mn(1) edge for **2** are 10.758, 10.758, and 10.876 Å, respectively (Figure S1).

The structure for **1** comprises a corrugated 2-D cyano-bridged array. Interestingly, the layers interact by pairs defining bilayers (Figure 3). The cohesive force in the bilayer networks from strong argentophilic interactions. The average Ag...Ag distance in the bilayers is 3.208 Å, less than the sum of the van der Waals radii of Ag (3.60 Å). The distances between two consecutive non-interacting layers are notably larger. The space between the 2D Mn(NCAgCN–Mn_{1/4})₄ host frameworks is filled with the 3-methylpyridine. On the other hand, the structure for **2** is doubly interpenetrating, as shown in Figure 4.

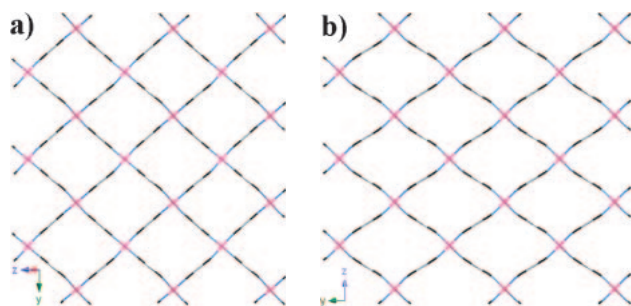


Figure 1. The cylinder drawing, 2-D structure of **1** (a) and **2** (b). Atom code: Mn(purple), Ag(white), N(blue), C(black). In this picture, hydrogen atoms, 3-methylpyridine, and 4-methylpyridine are omitted for clarity.

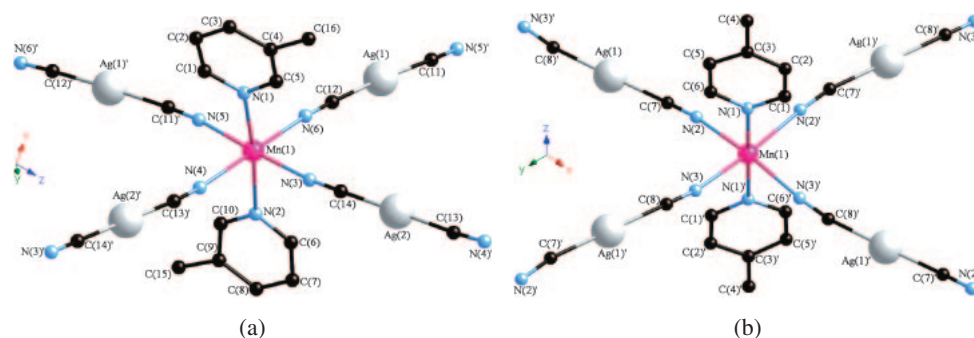


Figure 2. Coordination structure of the Mn and Ag ions in **1** (a) and **2** (b). In this picture, hydrogen atoms are omitted for clarity.

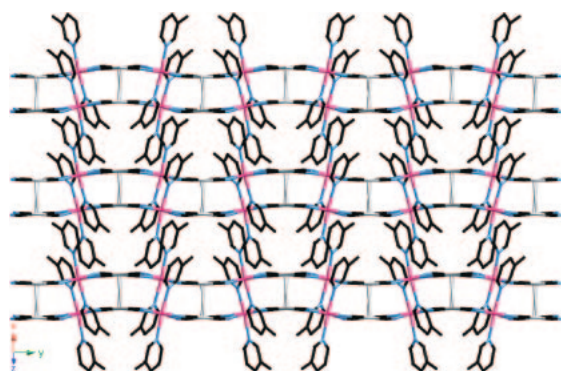


Figure 3. Stacking of consecutive bilayers of **1** with strong argentophilic interactions. In this picture, hydrogen atoms are omitted for clarity.

The closest approach between networks corresponds to weak argentophilic Ag...Ag interactions (3.341 Å), which define zigzag-chain Ag arrangements (Figure 5). Such a zigzag-chain structure is unprecedented for Hofmann-like cyano-bridged coordination polymers. Furthermore, we note that 4-methylpyridine rings of **2** are involved in a parallel displaced π – π stacking interaction. The centroids of the 4-methylpyridine rings are separated by 3.479 Å. The mode of 1D infinite π – π stacking is displayed in Figure 6. The interaction is weak in nature.¹⁷

Magnetic Properties. $\chi_M T$ versus T and χ_M^{-1} versus T plots, with χ_M being the molar magnetic susceptibility and T the temperature, for **1** and **2** are shown in Figures S2 and S3. At room temperature, the magnetic behaviors of the complexes **1** and **2** are characteristic of Mn^{II} compounds in the high-spin state, $\chi_M T = 4.11$ (**1**), $4.30 \text{ cm}^3 \text{ K mol}^{-1}$ (**2**) and the values of μ_{eff} are ($\mu_{\text{eff}} = 2.828\sqrt{\chi_M T}$) of **1** and **2** per one Mn^{II} ion at 300 K were 5.73, and $5.86 \mu_B$, respectively. The values for **1** and **2** are slightly smaller than $5.92 (=g\sqrt{S(S+1)})$, $g = 2$, $S = 5/2$ that of a pure spin only system, whereas the values are similar to the μ_{eff} value at 300 K of other Mn^{II} compounds.¹⁸ The magnetic values could be fitted with the Curie–Weiss equation $\chi_M = C/(T - \theta)$, where $C = 4.11 \text{ emu K mol}^{-1}$ and $\theta = -0.26 \text{ K}$ for **1** and $C = 4.32 \text{ emu K mol}^{-1}$ and $\theta = -0.07 \text{ K}$ for **2**. These slightly negative θ values seem consistent with very weak antiferromagnetic interaction between two Mn^{II} atoms with $S = 5/2$ spins bridged by a $[\text{Ag}(\text{CN})_2]^-$ unit. For both complexes, the $\chi_M T$ values were nearly constant in the range of 15–300 K; however, they

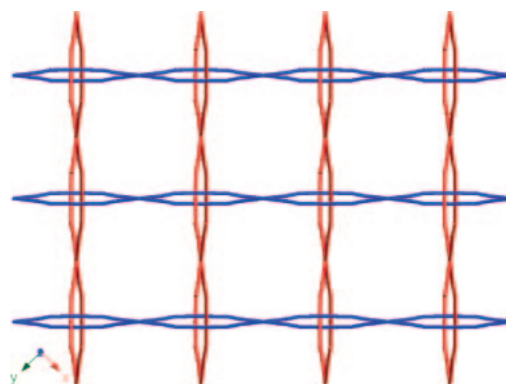


Figure 4. The cylinder drawing, doubly interpenetrated 2-D-networks of **2**.

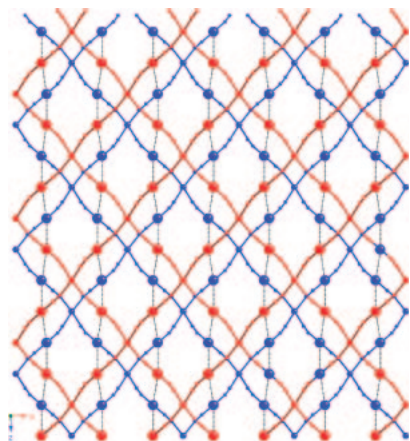


Figure 5. Doubly interpenetrated networks of **2** with weak 1D argentophilic interactions (black dotted line) among the networks.

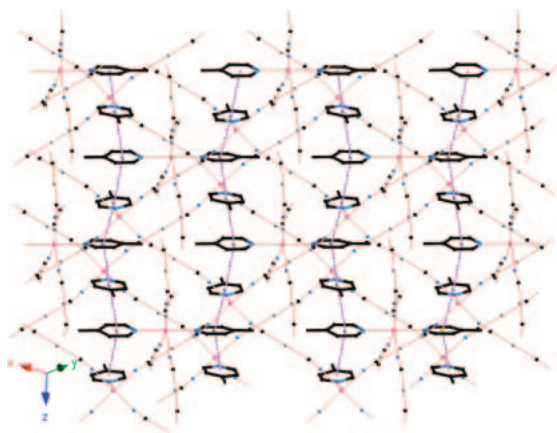


Figure 6. View of 1D infinite π - π stacking interactions (purple dotted line) in the complex **2**. In this picture, hydrogen atoms are omitted for clarity.

decreased as the temperature was lowered to less than 15 K. The decrease in the values of $\chi_M T$ at lower temperature is due to zero-field splitting (ZFS) effects of the sextuplet spin state of the metallic Mn^{II} centers in the HS species.^{19–21} In general, for Mn^{II} ions, ZFS is small. Nevertheless, in **1** and **2**, ZFS may be important, because the octahedral coordination geometries of the Mn^{II} ions in **1** and **2** are distorted.

Conclusion

In the current study, we synthesized novel bimetallic polycrystalline coordination compounds with the formula $\{Mn^{II}(L)_2[Ag^I(CN)_2]_2\}_n$ (L = 3-methylpyridine (**1**) or 4-methylpyridine (**2**)). In complex **1** and **2**, Mn^{II} and Ag^I atoms constitute the building blocks of these structures. The quasi-linear bidentate $[Ag(CN)_2]^-$ bridges Mn^{II} atoms, assemble to form a similar large $\{Mn^{II}_2[Ag^I(CN)_2]_4\}$ rectangular mesh 2D network. However, these complexes are structural isomers. The structure of **1** comprises parallel 2D array and the 2D layers are organized in pairs, in which strong binuclear argentophilic interactions hold them together. On the other hand, double interpenetration occurs in **2** and the attraction between 2D networks corresponds to weak argentophilic interactions, which

create Ag zigzag-chain arrangements.

From the measurements of the temperature dependence of the magnetic susceptibility, the profile of the magnetic behaviors of the complexes **1** and **2** are characteristic of Mn^{II} compounds in the high-spin state with ZFS.

In many dicyanometalates complexes, the introduction of $[M'(CN)_2]^-$ (M = Ag and Au) plays an important role as a bridging ligand between metal atoms (e.g., Mn, Fe, Co, Cd, etc.) to form multi-dimensional structures, such as 1D chains,^{10,22} 2D layers,^{1,3,11} and 3D frameworks,^{4–7,9,13} including **1** and **2** in this study. From the standpoint of crystal engineering, these fact suggest that structural control to form multi-dimensional structures involving $-NC-M-CN-$ linkages between M' atoms with the secondary ligands is delicate work and that the construction of supramolecular coordination architecture should give rise to unexpected crystal packing or inclusion structures. It may be possible to prepare analogous Fe^{II} compounds, which may have interesting magnetic properties, such as spin-crossover phase transition and molecular magnetism. These novel Mn^{II} coordination polymers should be useful as crystalline model compounds for studying spin crossover in analogous Fe^{II} compounds and for controlling coordination metal-organic frameworks on the nanoscale level. The increasing interest in metal-organic frameworks arises not only from their intrinsic beauty, but also from their potential applications. Therefore, this simple synthetic method for the preparation of multi-dimensional complexes might be useful for generating a variety of functional complexes.

Supporting Information

Figures S1, S2, and S3 show the cylinder drawing, one-dimensional wave chain edge structure of **1** and **2**, the magnetic properties of **1** and **2**, and the magnetic plot for the best-fit calculation of Curie-Weiss law on **1** and **2**. This material is available free of charge on the Web at: <http://www.csj.jp/journals/bcsj/>.

References

- 1 a) T. Soma, T. Iwamoto, *J. Inclusion Phenom. Mol. Recognit. Chem.* **1996**, 26, 161. b) T. Soma, T. Iwamoto, *Chem. Lett.* **1994**, 821.
- 2 T. Kitazawa, Y. Gomi, M. Takahashi, M. Takeda, M. Enomoto, A. Miyazaki, T. Enoki, *J. Mater. Chem.* **1996**, 6, 119.
- 3 a) T. Kitazawa, T. Kawasaki, M. Takahashi, M. Takeda, *KURRI-KR* **2004**, 106, 1. b) J. A. Rodríguez-Velamazán, M. Castro, E. Palacios, R. Burriel, T. Kitazawa, T. Kawasaki, *J. Phys. Chem. B* **2007**, 111, 1256. c) T. Kosone, C. Kachi-Terajima, C. Kanadani, T. Saito, T. Kitazawa, *Chem. Lett.* **2008**, 37, 422. d) T. Kitazawa, A. Suzuki, T. Kosone, *KURRI-KR* **2008**, 136, 50. e) T. Kosone, C. Kachi-Terajima, C. Kanadani, T. Saito, T. Kitazawa, *Chem. Lett.* **2008**, 37, 754.
- 4 V. Niel, M. C. Muñoz, A. B. Gasper, A. Galet, G. Levchenko, J. A. Real, *Chem.—Eur. J.* **2002**, 8, 2446.
- 5 a) D. B. Leznoff, B.-Y. Xue, C. L. Stevens, A. Storr, R. C. Thompson, B. O. Patrick, *Polyhedron* **2001**, 20, 1247. b) D. B. Leznoff, J. Lefebvre, *Gold Bull.* **2005**, 38, 47.
- 6 A. Galet, V. Niel, M. C. Muñoz, J. A. Real, *J. Am. Chem. Soc.* **2003**, 125, 14224.
- 7 V. Niel, A. L. Thompson, M. C. Muñoz, A. Galet, A. E. Goeta, J. A. Real, *Angew. Chem., Int. Ed.* **2003**, 42, 3760.

- 8 a) Z. J. Zhong, H. Seino, Y. Mizobe, M. Hidai, A. Fujishima, S. Ohkoshi, K. Hashimoto, *J. Am. Chem. Soc.* **2000**, *122*, 2952. b) J. J. Sokol, A. G. Hee, J. R. Long, *J. Am. Chem. Soc.* **2002**, *124*, 7656.
- 9 T. Soma, H. Yuge, T. Iwamoto, *Angew. Chem., Int. Ed. Engl.* **1994**, *33*, 1665.
- 10 I. P. Y. Shek, W.-Y. Wong, T.-C. Lau, *New J. Chem.* **2000**, *24*, 733.
- 11 E. Colacio, F. Lloret, R. Kivekäs, J. Ruiz, J. Suárez-Varela, M. R. Sundberg, *Chem. Commun.* **2002**, 592.
- 12 P. Pyykkö, *Chem. Rev.* **1997**, *97*, 597.
- 13 W. Dong, Q.-L. Wang, S.-F. Si, D.-Z. Liao, Z.-H. Jiang, S.-P. Yan, P. Cheng, *Inorg. Chem. Commun.* **2003**, *6*, 873.
- 14 a) A. Galet, M. C. Muñoz, V. Martínez, J. A. Real, *Chem. Commun.* **2004**, 2268. b) M. C. Muñoz, A. B. Gaspar, A. Galet, J. A. Real, *Inorg. Chem.* **2007**, *46*, 8182. c) G. Agustí, M. C. Muñoz, A. B. Gaspar, J. A. Real, *Inorg. Chem.* **2008**, *47*, 2552.
- 15 G. M. Sheldrick, *SADABS, Program for Empirical Absorption Correction for Area Detector Data*, University of Göttingen, Göttingen, Germany, **1996**.
- 16 G. M. Sheldrick, *SHELXL, Program for the Solution of Crystal Structures*, University of Göttingen, Göttingen, Germany, **1997**.
- 17 a) C. Janiak, *J. Chem. Soc., Dalton Trans.* **2000**, 3885. b) D. L. Reger, J. R. Gardinier, R. F. Semeniuc, M. D. Smith, *Dalton Trans.* **2003**, 1712. c) D. L. Reger, R. F. Semeniuc, M. D. Smith, *Cryst. Growth Des.* **2005**, *5*, 1181.
- 18 T. Kawasaki, C. Kachi-Terajima, T. Saito, T. Kitazawa, *Bull. Chem. Soc. Jpn.* **2008**, *81*, 268.
- 19 D. M. L. Goodgame, H. El Mkami, G. M. Smith, J. P. Zhao, E. J. L. McInnes, *Dalton Trans.* **2003**, 34.
- 20 S. Naskar, D. Mishra, S. K. Chattopadhyay, M. Corbella, A. J. Blake, *Dalton Trans.* **2005**, 2428.
- 21 C. Duboc, T. Phoeung, S. Zein, J. Pécaut, M.-N. Collomb, F. Neese, *Inorg. Chem.* **2007**, *46*, 4905.
- 22 I. Dasna, S. Golhen, L. Ouahab, N. Daro, J.-P. Sutter, *Polyhedron* **2001**, *20*, 1371.